# Diffractive deep inelastic scattering from the generalized BFKL pomeron. Predictions for HERA

M. Genovese

*Dipartimento di Fisica Teorica, Università di Torino, and INFN, Sezione di Torino, Via P. Giuria 1, I-10125 Torino, Italy*

N. N. Nikolaev and B. G. Zakharov

*IKP(Theorie), KFA Jülich, 5170 Jülich, Germany; L. D. Landau Institute for Theoretical Physics, GSP-1, 117940 ul. Kosygina 2, Moscow V-334, Russia*

We present microscopic QCD calculation of the cross-section of diffractive deep inelastic scattering (DIS) and of the partonic structure of the pomeron from the dipole approach to the generalized BFKL pomeron. We carry out a detailed analysis of how one can factor out the nonperturbative normalization of the diffractive DIS cross-section and its $Q^2$-evolution, which can be cast in the form of the conventional QCD evolution. We demonstrate that the pomeron cannot be treated as a particle with uniquely defined structure function and flux in the proton. We find strong factorization breaking which can approximately be described by the two-component structure function of the pomeron, each component endowed with a different flux of pomerons in the proton. We predict that the diffractive contribution to the proton structure function has very weak $Q^2$-dependence. © *1995 American Institute of Physics.*

## 1. INTRODUCTION

Much progress in our understanding of the QC pomeron is expected from experiments on inclusive diffractive deep inelastic scattering (DIS) $\gamma^* + p \rightarrow X + p'$ in progress at HERA. Extrapolating the Regge theory considerations[1] and assuming single-pomeron exchange, one can alternatively view this process as DIS on pomerons radiated by protons. This analogy inspired suggestions,[2,3] although conspicuously short of a microscopic QCD derivation, that the pomeron be treated as a particle with a well defined partonic structure. Understanding the accuracy, and limitations, of such a partonic description of diffractive DIS is a topical issue which we address here in the framework of the microscopic dipole cross-section approach to the generalized BFKL pomeron.[4–6] Our principal conclusion is that, in the subasymptotic kinematical region accessible at HERA, this is only possible at the expense of a two-component partonic structure of the pomeron, which leads to specific breaking of the conventional parton-model factorization.

We consider DIS for

$$x = \frac{Q^2}{Q^2 + W^2} \ll 1$$

followed by diffraction excitation of the virtual photon into the state $X$ of mass $M$, where $Q^2$ is the virtuality of the photon and $W$ is the total energy in the photon-proton center of mass. The variable

$$x_{\mathrm{P}} = \frac{M^2 + Q^2}{W^2 + Q^2} \ll 1$$

can be interpreted as the fraction of the proton momentum taken away by the pomeron, and

$$\beta = \frac{x}{x_{\mathrm{P}}} = \frac{Q^2}{Q^2 + M^2}$$

is the Bjorken variable for DIS on the pomeron. The final-state proton $p'$ carries a fraction $1 - x_{\mathrm{P}}$ of the momentum of the beam proton and is separated from the hadronic debris $X$ of the photon by the (pseudo) rapidity gap

$$\Delta \eta \approx \log \frac{1}{x_{\mathrm{P}}} \gtrsim \Delta \eta_c \gtrsim (2.5 - 3).$$

Once the total cross-section of photoabsorption on the pomeron $\sigma_{\mathrm{tot}}(\gamma^* \mathrm{P}, M^2)$ is known, the pomeron structure function can be defined operationally by the standard formula

$$F_2^{(\mathrm{P})}(x, Q^2) = \frac{Q^2}{4\pi^2 \alpha_{em}} \alpha_{\mathrm{tot}}(\gamma^* \mathrm{P}, M^2),$$

where $\alpha_{em}$ is the fine-structure constant. Extension of the Regge theory convention[1] to DIS gives the operational definition[5]

$$\alpha_{\mathrm{tot}}(\gamma^* \mathrm{P}, M^2) = \frac{16\pi}{\sigma_{\mathrm{tot}}(pp)} (M^2 + Q^2) \times \frac{d\sigma_D(\gamma^* + p \rightarrow X + p)}{dt\, dM^2}\Bigg|_{t=0} \quad (1)$$

in terms of the experimentally measured cross-section of diffractive DIS, where $t$ is the $(p, p')$ momentum transfer squared. This convention implicitly assumes that total cross-section is asymptotically constant, i.e., the flux of pomerons in the proton $f_{\mathrm{P}}(x_{\mathrm{P}})/x_{\mathrm{P}}$ satisfies $f_{\mathrm{P}}(x_{\mathrm{P}}) = 1$. Finally, the gen-

eralization of (1) to DIS, under the strong assumption of factorization of the flux and structure function of pomerons, is[1]

$$(M^2+Q^2)\left.\frac{d\sigma_D(\gamma^*\to X)}{dt\, dM^2}\right|_{t=0} = x_{\mathrm{P}}\left.\frac{d\sigma_D(\gamma^*\to X)}{dt\, dx_{\mathrm{P}}}\right|_{t=0}$$

$$= \frac{\sigma_{\mathrm{tot}}(pp)}{16\pi}\frac{4\pi^2\alpha_{em}}{Q^2}f_{\mathrm{P}}(x_{\mathrm{P}})F_2^{(\mathrm{P})}(\beta,Q^2), \qquad (2)$$

where $\sigma_{\mathrm{tot}}(pp)=40$ mb is an energy-independent dimensional normalization constant and $\alpha_{em}$ is the fine-structure constant.

Evidently, the above set of operational definitions only makes sense if the pomeron flux function $f_{\mathrm{P}}(x_{\mathrm{P}})$ can be defined in such a way that the $Q^2$-dependence of the r.h.s. of (2) is concentrated in $F_2^{\mathrm{P}}(\beta,Q^2)$, which satisfies the conventional QCD evolution. This factorization (convolution) property (2) and the QCD evolution property of $F_2^{\mathrm{P}}(\beta,Q^2)$ must be proven starting with the microscopic QCD treatment of diffractive DIS, rather than be postulated, and in this paper we address this issue in the framework of the dipole cross-section reformulation[5,6] of the BFKL pomeron[7] (the somewhat related dipole approach is also discussed in Ref. 8). In this dipole BFKL approach, the convolution representation (2) is problematical for several reasons. For instance, at subasymptotic energies, the dipole pomeron does not factor,[5,6] and the recent BFKL phenomenology of DIS has shown[9] that the kinematical domain of HERA is the subasymptotic one. The naive partonic description of the pomeron was shown to fail in diffractive jet production.[4,10] Furthermore, in the approximation $\alpha_S=$const and in the asymptotic BFKL regime $1/x_{\mathrm{P}}$, $1/\beta\to\infty$, the description of diffractive DIS can change: there is a possibility of mixing of the two- and four-gluon states for the cut pomeron while retaining two-gluon structure of the exchanged BFKL pomerons.[11]

However, even at the high energy of HERA, because of the important kinematical relationship $x=x_{\mathrm{P}}\beta$ neither $x_{\mathrm{P}}$ nor $\beta$ can be made asymptotically small (hereafter we consider $x_{\mathrm{P}}\leq x_{\mathrm{P}}^0 = 0.03$). We recall that in the scenario[6,9,12] for the dipole BFKL pomeron, the difference between the BFKL and GLDAP descriptions of the proton structure functions remains marginal down to $x\gtrsim 10^{-6}$.[9] Because the experimentally accessible $\beta$ is not very small, we start our analysis with the Born approximation for diffractive DIS. By virtue of the relationship between diffraction excitation of Fock states of the photon and the partonic components of the pomeron, these Born cross-sections define the nonperturbative input valence $q\bar{q}$ and the gluon structure functions of the pomeron and the nonperturbative fluxes of pomerons in the proton. Again, because of the moderately small $\beta$, excitation of higher Fock states of the photon is dominated by the size ordering of partons equivalent to the familiar leading-log $Q^2$ approximation (LLQA).[5] It is precisely this LLQA which enables us to reinterpret the contribution from excitation of higher Fock states to the cross-section of diffractive DIS as GLDAP evolution[13] of the two-component pomeron structure function starting with the nonperturbative input valence $q\bar{q}$ and gluon distributions of the Born approximation, respectively. We demonstrate that the convolution (2) indeed

breaks down, because the two components of the pomeron structure function must be endowed with fluxes of pomerons in the proton which are different for the subasymptotic properties of the dipole cross-section.

The further presentation is organized as follows. In Sec. 2 we derive the valence $q\bar{q}$ structure function of the pomeron and the corresponding flux of pomerons $\phi_{\mathrm{P}}(x_{\mathrm{P}})$ is the proton. In Sec. 3 we derive the sea structure function of the pomeron and the corresponding flux $f_{\mathrm{P}}(x_{\mathrm{P}})$, which is different from $\phi_{\mathrm{P}}(x_{\mathrm{P}})$. In Sec. 4 we formulate the two-component description of the pomeron structure function and discuss the breaking of the factorization (2). Predictions for the diffractive contribution $F_2^D(x,Q^2)$ to the proton structure function are presented in Sec. 5. In the Conclusions section we summarize our major results.

## 2. THE VALENCE $q\bar{q}$ COMPONENT OF THE POMERON

The approach[4,5] starts with the microscopic calculation of $d\sigma_D/dtdM^2|_{t=0}$ and a thorough examination of whether it can be reinterpreted, via Eqs. (1), (2), in terms of a GLDAP evolving pomeron structure function or not. The Born cross-section for diffraction excitation of the $q\bar{q}$ Fock state of the photon equals (hereafter we focus on the dominant diffraction dissociation of transverse photons)

$$\left.\frac{d\sigma_D(\gamma^*\to X)}{dt}\right|_{t=0} = \int dM^2 \left.\frac{d\sigma_D(\gamma^*\to X)}{dtdM^2}\right|_{t=0}$$

$$= \frac{1}{16\pi}\int_0^1 dz\int d^2\mathbf{r}|\Psi_{\gamma}*(Q^2,z,r)|^2\sigma^2(x,r)$$

$$= \frac{4\pi^2\alpha_{em}}{Q^2}\int\frac{dr^2}{r^2}W(Q,r)\left[\frac{\sigma(x,r)}{r^2}\right]^2. \qquad (3)$$

Here $\mathbf{r}$ is the transverse separation of the quark and antiquark in the photon, $z$ and $1-z$ are partitions of the lightcone momentum of the photon between the quark and antiquark, $\sigma(x,r)$ is the dipole cross-section for scattering on the proton target (hereafter we use $\sigma(x,r)$ of Refs. 9, 12), and the dipole distribution in the photon $|\Psi_{\gamma}*(Q^2,z,r)|^2$ derived in Ref. 14 equals

$$|\Psi_{\gamma}*(Q^2,z,r)|^2 = \frac{6\alpha_{em}}{(2\pi)^2}\sum_i^{N_f} e_i^2\{[z^2+(1-z)^2]$$

$$\times\varepsilon^2 K_1(\varepsilon r)^2+m_i^2K_0(\varepsilon r)^2\}, \qquad (4)$$

where $e_i$ is the quark charge in units of the electron charge, $m_i$ is the quark mass, $\varepsilon^2=z(1-z)Q^2+m_i^2$

and $K_\nu(x)$ is a modified Bessel function of the second kind. Precisely the same dipole cross-section enters the calculation of the proton structure function
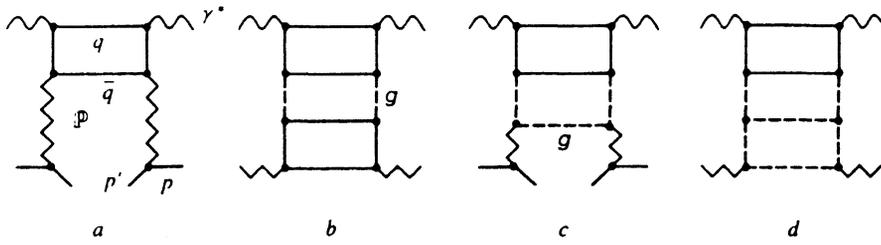
FIG. 1. The diffraction excitation diagrams describing DIS on (a) valence $q\bar{q}$ state of the pomeron; (c) the valence-glue generated sea of the pomeron; and (b,d) the $Q^2$-evolution effects.

$F_2^p(x,Q^2)$

$$= \frac{Q^2}{4\pi^2 \alpha_{em}} \int_0^1 dz \int d^2 \mathbf{r} |\Psi_{\gamma *}(Q^2,z,r)|^2 \sigma(x,r),$$

(5)

and the scenario[9,12] for $\sigma(x,r)$ was shown[9] to give a good quantitative description of the HERA data[15] in the whole region of $x$ and $Q^2$.

The ingredients which allow reinterpretation of the cross-section (3) as DIS on the valence $q\bar{q}$ state of the pomeron are: 1) the mass spectrum calculated in Ref. 4, which roughly follows

$$\frac{d\sigma_D}{dM^2 dt}\bigg|_{t=0} \propto \frac{M^2}{(Q^2+M^2)^3} = \frac{1}{Q^2}\frac{1}{Q^2+M^2}\beta(1-\beta), \quad (6)$$

is $x$-independent to a good approximation; 2) at large $Q^2$ the weight function $W(Q,r)$ is $Q^2$-independent and the diffractive cross-section $\sigma_D(\gamma^* \to q\bar{q})$ satisfies the Bjorken scaling;[4,14] 3) the weight function $W(Q,r)$ is peaked at large, and $Q^2$-independent, hadronic size $r = R_{val} \sim 1/m_q$. This greatly resembles the $Q^2$-independent large spatial separation of the valence quark and antiquark in the pion, and we can analogously speak of DIS off the valence $q\bar{q}$ state of the pomeron.

The corollary of the above is that in Eq. (3) the $x$ and $\beta$ dependence can be factored and we can write down the convolution representation

$$x_P \frac{d\sigma_D(\gamma^* \to q\bar{q})}{dt\, dx_P}\bigg|_{t=0} = \frac{\sigma_{tot}(pp)}{16\pi}$$

$$\times \frac{4\pi^2 \alpha_{em}}{Q^2} \phi_P(x_P)F_{val}^P(\beta), \quad (7)$$

in which the valence $q\bar{q}$ structure function of the pomeron

$$F_{val}^{(P)}(\beta) = C_{val}\beta(1-\beta) = 0.27\beta(1-\beta) \quad (8)$$

follows from the mass spectrum (6) (Ref. 4, see also Ref. 3). The flux function $\phi_P(x_P)$, defined subject to the normalization $\phi_P(x_P^0) = 1$, equals

$$\phi_P(x_P) = \frac{\int_0^1 dz \int d^2 \mathbf{r} |\Psi_{\gamma *}(Q_P^2,z,r)|^2 \sigma^2(x_P,r)}{\int_0^1 dz \int d^2 \mathbf{r} |\Psi_{\gamma *}(Q_P^2,z,r)|^2 \sigma^2(x_P^0,r)}. \quad (9)$$

As long as the factorization scale $Q^2 = Q_P^2$ is chosen large enough, so that $Q_P^2 \gg 1/R_{val}^2$ holds, the flux function $\phi_P(x_P)$ will not depend on $Q_P^2$; for the choice of $Q_P^2$ see below. Because in DIS on the valence (anti)quarks $\beta \sim 1$ [Eq. (8)],

for $x \ll 1$ we can neglect the distinction between $\phi_P(x)$ and $\phi_P(x_P=x/\beta)$ in (7). Consequently, the diffractive DIS cross-section of Eq. (7) satisfies the Bjorken scaling and has the desired convolution form. Fig. 1a gives an abridged summary of the above analysis; the factor $\sigma^2(x,r)$ in (3) is an exact result of the calculation of 16 Feynman diagams with all the possible couplings of the two gluons of each pomeron to the excited $q\bar{q}$ pair.[4,5,14]

Both the normalization $C_{val}$ of $F_{val}^P(\beta)$ and the $x_P$-dependence of the pomeron flux function $\phi_P(x_P)$ are controlled by $\sigma(x,r)$ at the large, nonperturbative, dipole size $r \sim 1/m_q$. At moderately small $x_P$, this cross-section is not perturbatively calculable and rather must be inferred from an analysis of the experimental data in the same dipole cross section approach. Here we wish to emphasize that the similar dipole size enters the calculation of the real photoabsorption cross-section[15] and nuclear shadowing in DIS,[16,18] which are well reproduced with the choice $m_q = 0.15$ GeV. The flux function $\phi_P(x_P)$ is shown in Fig. 2. The absolute normalization of the valence of the pomeron, $C_{val}=0.27$, in (8) is fixed
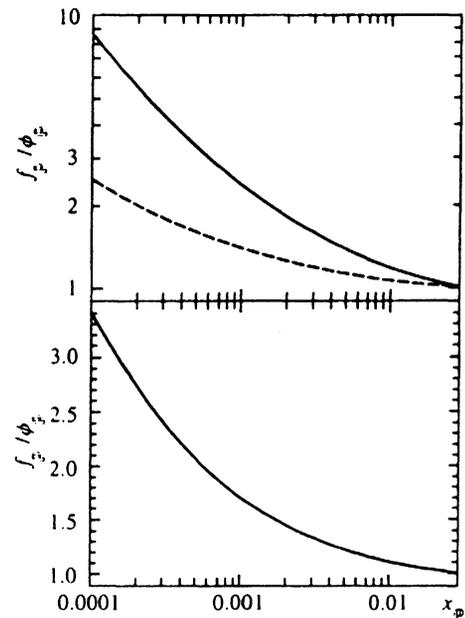


FIG. 2. Predictions from the dipole BFKL pomeron for flux functions $\phi_P(x_P)$ (dashed curve) and $f_P(x_P)$ (solid curve) for the $F_{val}^P(\beta,Q^2)$ and $F_{sea}^P(\beta,Q^2)$ components of the pomeron structure function, respectively, and the ratio of the two fluxes (the bottom box).
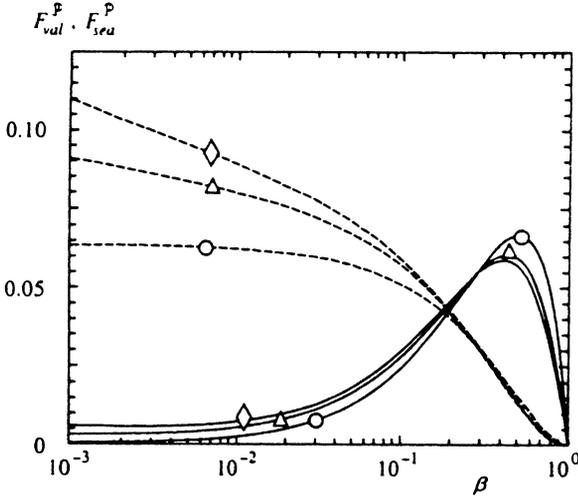
$F^{P}_{val}, F^{P}_{sea}$



FIG. 3. Predictions from the dipole BFKL pomeron for the $Q^2$-evolution of components $F_{val}(\beta,Q^2)$ (solid curves) and $F^{P}_{sea}(\beta,Q^2)$ (dashed curves) of the pomeron structure function for $Q^2 = 10$ (O), 50 ($\triangle$), 100 ($\diamond$) GeV$^2$.

by requiring that the convolution (7) give the same $q\bar{q}$ excitation cross-section as formula (3). The flavor decomposition of valence parton distribution $v_i(\beta) = A_i(1-\beta)$ is $A_u = A_{\bar{u}} = A_d = A_{\bar{d}} = 0.20, A_s = A_{\bar{s}} = 0.11, A_c = A_{\bar{c}} = 0.02$ (for a discussion of the flavour asymmetry of diffractive DIS see Ref. 4).[2] A conservative estimate of the uncertainty in $\sigma(x_P, r \sim 1/m_q)$ is $\lesssim 15$–20%, and the uncertainty in our prediction for $C_{val}$ is $\lesssim 30\%$. These valence distributions can be used as an input at $Q^2 = Q^2_P = 10$ GeV$^2$ (this choice is discussed below) for the GLDAP evolution of $F^{P}_{val}(\beta,Q^2)$, which sums the higher order diagrams of Fig. 1(b), describing the sea originating from the pure valence $q\bar{q}$ pomeron. Here the crucial point discussed to great detail in Ref. 5 is that at the moderately small $\beta$ of interest in the present paper, the LLQA ordering in sizes dominates the diffractive DIS of higher Fock states of the photon, which is the standard condition for the GLDAP evolution. The predicted $Q^2$-dependence of $F^{P}_{val}(\beta,Q^2)$ is shown in Fig. 3. In conformity with experience with the proton structure function at moderately small $x$, the $Q^2$-evolution effects are small.

## 3. VALENCE GLUONS AND SEA IN THE POMERON

The mass spectrum (6) for excitation of the $q\bar{q}$ state rapidly decreases at large $M^2 \gg Q^2$. The Born process for the mass spectrum $\propto 1/(M^2 + Q^2)$, typical of the so-called triple-pomeron regime,[1,17] is diffraction excitation of the $q\bar{q}g$ Fock state of the photon.[5] The new nonperturbative parameter which emerges in the lightcone description of the $q\bar{q}g_1 \ldots g_n$ Fock states of the photon is the correlation (propagation) radius $R_c = 1/\mu_G$ for the perturbative gluons. Following lattice QCD studies,[18] we take $R_c \approx 0.27$ fm ($\mu_G = 0.75$ GeV).[6,9] According to the analysis,[5] for large $Q^2 \gg 1/R^2_c$ diffraction excitation $\gamma^* \to q\bar{q}g$ is dominated by the LLQA configurations in which the $q\bar{q}$ separation $r \sim 1/\sqrt{Q^2}$ is much smaller than the $qg, \bar{q}g$ separation $\rho$. Because of this LLQA ordering of sizes

$$(Q^2 + M^2) \frac{d\sigma_D}{dt\, dM^2}\bigg|_{t=0} \approx \int dz\, d^2\mathbf{r} |\Psi_{\gamma*}(Q^2, z, r)|^2$$

$$\times \frac{16\pi^2}{27} \alpha_S(r) r^2 \frac{1}{2\pi^4} \left(\frac{9}{8}\right)^3$$

$$\times \int d\rho^2 \left[\frac{\sigma(x^P, \rho)}{\rho^2}\right]^2 \mathscr{F}(\mu_G \rho)$$

(10)

with the factored $Q^2$- and $x_P$-dependence. Here $\alpha_S(r)$ is the running QCD coupling with freezing at large distances[6] and the form factor is

$$\mathscr{F}(z) = z^2 [K_1(z)^2 + z K_1(z) K_0(z) + \tfrac{1}{2} z^2 K_0(z)^2].$$

It is precisely this factorization property which allows us to define the corresponding structure function and the pomeron flux function.

It is convenient to introduce the dimensional normalization constant $A^*_{3P}$ such that

$$A^*_{3P} f_P(x_P) = \frac{1}{2\pi^4} \left(\frac{9}{8}\right)^3 \int dr^2 \left[\frac{\sigma(x_P, r)}{r^2}\right]^2 \mathscr{F}(\mu_G r), \quad (11)$$

where $f_P(x_P)$ is the corresponding flux function, subject to the normalization $f_P(x^0_P) = 1$. The constant $A^*_{3P} = 0.56$ GeV$^{-2}$ has a meaning, and a magnetic close to, that of the triple pomeron coupling $A_{3P}(Q^2)$ (for a more detailed discussion see Ref. 19). Furthermore, one can introduce the explicit two-gluon wave function of the pomeron[5]

$$|\Psi_P(\beta, \mathbf{r})|^2 = \frac{1}{f_P(x_P)} \frac{81}{8\pi^4} \frac{1-\beta}{\beta} \frac{1}{\sigma_{tot}(pp)}$$

$$\times \left[\frac{\sigma(x_P, r)}{r^2}\right]^2 \mathscr{F}(\mu_G r), \quad (12)$$

where $\mathbf{r}$ is the transverse separation of gluons in the pomeron and $\beta$ is the fraction of the pomeron momentum carried by a gluon. In the wave function (12), the $x_P$-dependence cancels out approximately, yielding the $x_P$-independent gluon structure function of the pomeron

$$G_P(\beta) = \beta g_P(\beta) = \beta \int d^2\mathbf{r} |\Psi_P(\beta, \mathbf{r})|^2 = A_G(1 - \beta). \quad (13)$$

Then, Eq. (10) gives the input sea structure function of the pomeron

$$F^{P}_{sea}(\beta \ll 1, Q^2_P) = C_{sea}$$

$$= \frac{16\pi A^*_{3P}}{\sigma_{tot}(pp)} \frac{Q^2_P}{4\pi^2 \alpha_{em}} \int_0^1 dz\, d^2\mathbf{r} |\Psi_{\gamma*}(Q^2_P, r, z)|^2$$

$$\times \frac{16\pi^2 r^2 \alpha_S(r)}{27}, \quad (14)$$

which to the order in $\alpha_S(r)$ at which one LLQA loop emerges, has[5] the correct QCD scaling violation for the sea structure function which evolves from the valence gluonic state:

$$F^{\mathrm{P}}_{\mathrm{sea}}(\beta,Q^2_{\mathrm{P}}) \propto \log\left[\frac{1}{\alpha_S(Q^2_{\mathrm{P}})}\right]. \tag{15}$$

Equation (12) gives the LLQA limit of the sum of all the 81 Feynman diagrams with all the possible coupling of the two gluons of each exchanged pomeron to the quark, antiquark and gluon of the $q\bar{q}g$ Fock state of the photon, including additional Feynman diagrams which describe the renormalization for the virtual radiative corrections (for a detailed discussion see Ref. 5). Fig. 1c gives an abridged description of the final LLQA result. The result (15) is the starting point of GLDAP evolution for moderately small $\beta$ when diffraction dissociation of higher Fock states is included.

The wave function (12) corresponds to a relatively small transverse size $r \sim R_{\mathrm{sea}} \approx R_c$ for the $gg$ state of the pomeron. In DIS on protons, the onset of GLDAP evolution requires $Q^2 \gtrsim Q^2_N \sim 2$ GeV$^2$.[20] Then we can argue that, in DIS on the pomeron, GLDAP evolution becomes applicable for $Q^2 \gtrsim Q^2_{\mathrm{P}} = Q^2_N(R_p/R_{\mathrm{sea}})^2$, which suggests the choice of the factorization scale for the pomeron $Q^2_{\mathrm{P}} = 10$ GeV$^2$.

In (12), the dependence $\propto 1/\beta$ is a usual soft-gluon behavior; the factor $1-\beta$ in (12) is an educated guess. In the limit $\beta \to 1$ it makes the two valence distributions (8) and (12) behave similarly, in the spirit of quark counting rules, and the $q\bar{q}$ sea contribution to the pomeron structure function behaves as $\sim(1-\beta)^2$. As a starting approximation we take

$$F^{\mathrm{P}}_{\mathrm{sea}}(\beta,Q^2_{\mathrm{P}}) = C_{\mathrm{sea}}(1-\beta)^2 = 0.063(1-\beta)^2 \tag{16}$$

with normalization which follows from Eq. (14) and differs only slightly from the earlier estimate.[4] The flavor decomposition of the input sea in the pomeron is

$$q^{(i)}_{\mathrm{sea}}(\beta,Q^2_{\mathrm{P}}) = \bar{q}^{(i)}_{\mathrm{sea}}(\beta,Q^2_{\mathrm{P}}) = A^{(i)}_{\mathrm{sea}}(1-\beta)^2,$$

where

$$A^{(u)}_{\mathrm{sea}} = A^{(d)}_{\mathrm{sea}} = 0.048, \quad A^{(s)}_{\mathrm{sea}} = 0.040, \quad A^{(c)}_{\mathrm{sea}} = 0.009.$$

Finally,

$$A_G = \int d^2\mathbf{r}\{\beta|\Psi_{\mathrm{P}}(\beta,\mathbf{r})|^2\}_{\beta=0} = \frac{128\pi}{9}\frac{A^*_{3\mathrm{P}}}{\sigma_{\mathrm{tot}}(pp)} = 0.28. \tag{17}$$

This fully specifies the (parameter-free) input for the $Q^2$-evolution of the pomeron structure function $F^{\mathrm{P}}_{\mathrm{sea}}(\beta,Q^2)$, which originates from the gluonic component of the pomeron. QCD evolution sums the diagrams of Figs. 1c and d; the result of evolution of $F^{\mathrm{P}}_{\mathrm{sea}}(\beta,Q^2)$ is shown in Fig. 3. In the region $\beta \lesssim 10^{-2} - 10^{-3}$ accessible at HERA, the $Q^2$-evolution effects are still rather weak. $F^{\mathrm{P}}_{\mathrm{sea}}(\beta,Q^2)$ takes over $F^{\mathrm{P}}_{\mathrm{val}}(\beta,Q^2)$ at $\beta \lesssim 0.2$, as was anticipated earlier.[4]

We estimated $C_{\mathrm{sea}}$ and $A_G$ in terms of the dipole cross-section at small but still nonperturbative $r \sim R_c$, which must be inferred from an analysis of the related experimental data, which was the subject of recent work.[4,12,21-23] These data include real photoproduction of the $J/\Psi$,[24] exclusive leptoproduction of the $\rho^0$ and $\phi^0$ mesons for $Q^2 \lesssim 10-20$ GeV$^2$ [25] and color transparency effects in the $J/\Psi$[26] and $\rho^0$[27] production on nuclei, which probe the (predominantly nonperturbative) dipole cross-section at $r \sim 0.5$ fm $\lesssim 2R_c$.[12,21-23] Real

and weakly virtual, $Q^2 \lesssim 10$ GeV$^2$, photoproduction of the open charm probes the (predominantly perturbative) dipole cross-section at $r \sim 1/m_c \sim R_c/2$.[9,12] The proton structure function $F^p_2(x,Q^2)$ probes the dipole cross-section over a broad range of radii from $r \sim 1$ fm down to $r \sim 0.02$ fm.[9,20] Successful quantitative description of the corresponding experimental data obtained in Refs. 9, 12, 21-23 implies that we know the dipole cross-section $\sigma(x_{\mathrm{P}},r \sim R_c)$ to a conservative uncertainty $\lesssim 15-20\%$, and our estimates for $C_{\mathrm{sea}}$ and $A_G$ have an accuracy $\lesssim 30\%$.

## 4. THE TWO-COMPONENT STRUCTURE FUNCTION OF THE POMERON AND FACTORIZATION BREAKING

The two fluxes $\phi_{\mathrm{P}}(x_{\mathrm{P}})$ and $f_{\mathrm{P}}(x_{\mathrm{P}})$ are not identical (Fig. 2), because their $x_{\mathrm{P}}$-dependence is dominated by $\sigma(x_{\mathrm{P}},r \sim R_{\mathrm{val}})$ and $\sigma(x_{\mathrm{P}},r \sim R_{\mathrm{sea}})$, respectively, the latter having a faster growth with $1/x_{\mathrm{P}}$.[6,9,12] In the region $10^{-3} \lesssim x_{\mathrm{P}} \lesssim 0.03$ of practical interest for the HERA experiments, both fluxes can be well approximated (to an accuracy of a few parts per thousand) by the ansatz

$$f_{\mathrm{P}}(x_{\mathrm{P}}),\phi_{\mathrm{P}}(x_{\mathrm{P}}) = \left(\frac{x^0_{\mathrm{P}}}{x_{\mathrm{P}}}\right)^{p_1}\left(\frac{x_{\mathrm{P}}+p_3}{x^0_{\mathrm{P}}+p_3}\right)^{p_2}, \tag{18}$$

with $p_1 = 0.259$, $p_2 = 0.2142$, $p_3 = 1.49 \cdot 10^{-3}$ for the flux $\phi_{\mathrm{P}}(x_{\mathrm{P}})$, and $p_1 = 0.58$, $p_2 = 0.48$, $p_3 = 2.3 \cdot 10^{-3}$ for the flux $f_{\mathrm{P}}(x_{\mathrm{P}})$. As a matter of fact, the above parameterizations give a viable description of the two fluxes to better than 10% accuracy even down to $x_{\mathrm{P}} = 10^{-4}$. The different $x_{\mathrm{P}}$-dependence of the two fluxes is a solid dynamical prediction from the subasymptotic BFKL pomeron, to be contrasted with conjectured forms of the universal flux pomerons.[2,3] Only at values $1/x_{\mathrm{P}} \gg 1$, well beyond the kinematical range of HERA, should the two fluxes have a similar $(1/x_{\mathrm{P}})$ dependence with the exponent $p_1 = 2\Delta_{\mathrm{P}} = 0.8$ for the exchange by bare, nonunitarized, BFKL pomerons.[6] This asymptotic regime is completely inaccessible at HERA. Nonetheless, it is interesting to notice that if the ansatz (18) is applied to approximate the calculated fluxes in the much broader range $10^{-5} \lesssim x_{\mathrm{P}} \lesssim 0.03$, then at one finds $p_1 = 0.569$, $p_2 = 0.4895$, $p_3 = 1.53 \cdot 10^{-3}$ for the flux $\phi_{\mathrm{P}}(x_{\mathrm{P}})$, and $p_1 = 0.741$, $p_2 = 0.586$, $p_3 = 0.8 \cdot 10^{-3}$ for the flux $f_{\mathrm{P}}(x_{\mathrm{P}})$. In this case, the exponents $p_1$ are closer to the asymptotic value $p_1 = 2\Delta_{\mathrm{P}} = 0.8$. Incidentally, in the HERA region of $10^{-3} \lesssim x_{\mathrm{P}} \lesssim 0.03$, the latter fits describe the fluxes $\phi_{\mathrm{P}}(x_{\mathrm{P}})$ and $f_{\mathrm{P}}(x_{\mathrm{P}})$ to better than a few percent accuracy.

With allowance for different fluxes for the two components of the diffraction dissociation cross-section, the resulting two-component convolution formula reads

$$x_{\mathrm{P}}\frac{d\sigma_D}{dt\,dx_{\mathrm{P}}}\bigg|_{t=0} = \frac{4\pi^2\alpha_{em}}{Q^2}\frac{\sigma_{\mathrm{tot}}(pp)}{16\pi}[\phi_{\mathrm{P}}(x_{\mathrm{P}})F^{\mathrm{P}}_{\mathrm{val}}(\beta,Q^2)$$

$$+ f_{\mathrm{P}}(x_{\mathrm{P}})F^{\mathrm{P}}_{\mathrm{sea}}(\beta,Q^2)]$$

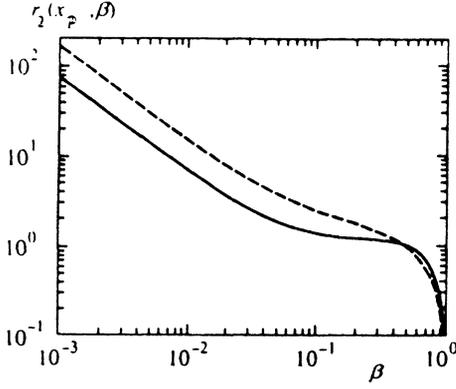$$= \frac{4\pi^2\alpha_{em}}{Q^2}\frac{\sigma_{\mathrm{tot}}(pp)}{16\pi}\Phi_D(x,\beta,Q^2,t=0). \tag{19}$$

FIG. 4. Predicted factorization breaking in the $\beta$ distribution $r_2(x_P,\beta)$ at $x_P=0.03$ (solid curve) and $x_P=0.0001$ (dashed curve). We take $\beta_0=0.5$ and $Q^2=25$ GeV$^2$.

It is convenient to study the factorization breaking in terms of the two ratios

$$r_1(\beta,x_P)=\frac{\Phi_D(x=x_P\beta,\beta,Q^2,0)}{\Phi_D(x=x_P^0,\beta,\beta,Q^2,0)}$$

and $r_2(x_P,\beta)=\dfrac{\Phi_D(x=x_P\beta,\beta,Q^2,0)}{\Phi_D(x=x_P\beta_0,\beta_0,Q^2,0)}$ (20)

and study their $x_P$- and $\beta$-dependence, varying $x$ at fixed $\beta$ and $x_P$, respectively. If the two fluxes were identical, $\phi_P(x_P)=f_P(x_P)$, then Eq. (19) would reduce to the naive parton model convolution (2) with the consequence that $r_1(\beta,x_P)=f_P(x_P)$ would be independent of $\beta$, whereas $r_2(x_P,\beta)$ would be independent of $x_P$. Our two-component picture predicts a strong factorization breaking,

$$r_1(\beta\gtrsim0.3,x_P)\approx\phi_P(x_P)\neq r_1(\beta\ll0.1,x_P)\approx f_P(x_P),$$
(21)

with $f_P(x_P)$ departing from $\phi_P(x_P)$ by a factor $\sim3.5$ ($\sim1.7$) as $x_P$ decreases from $x_P=0.03$ down to $x_P=10^{-4}$ ($x_P=10^{-3}$) (Fig. 2). Such strong factorization breaking must easily be observable at HERA with the next generation of data. Similarly, the results from our two-component picture for $r_2(x_P=0.03,\beta)$ and $r_2(x_P=0.0001,\beta)$ show a large factorization breaking, by the factor $\sim2.2$ (Fig. 4) at $\beta<0.1$, which also must be observable at HERA.

Above we focused on forward diffraction dissociation, $t=0$. At small $|t|$ within the diffraction peak, which is still dominated by single-pomeron exchange,

$$\Phi_D(x,\beta,Q^2,t)=\phi_P(x_P)F_{val}^P(\beta,Q^2)\exp(-B_{el}|t|)$$

$$+f_P(x_P)F_{sea}^P(\beta,Q^2)\exp(-B_{3P}|t|).$$
(22)

In Refs. 4, 5, 14 we argued that excitation of the $q\bar{q}$ valence of the pomeron is the counterpart of diffraction production of resonances in hadronic scattering and/or real photoproduction when it is appropriate to use the diffraction slope $B_{el}$ of elastic $\pi N$ scattering, whereas excitation of the sea of the pomeron is the counterpart of the triple-pomeron regime with $B_{3P}\sim B_{el}/2$. The hadronic and real photoproduction

data given $B_{3P}\approx6$ GeV$^{-2}$ [17,28] to $\lesssim25\%$. This guess for the slopes can be checked at HERA when ZEUS and H1 leading proton spectrometers will be in operation. Because of the different $t$-dependence of $\phi_P(x_P)\exp(-B_{el}|t|)$ and $f_P(x_P)\exp(-B_{3P}|t|)$ we predict a $t$-dependent factorization breaking. Finally, the $t$-integrated mass spectrum equals

$$x_P\frac{d\sigma_D}{dx_P}=\frac{4\pi^2\alpha_{em}}{Q^2}\frac{\sigma_{tot}(pp)}{16\pi B_{3P}}\left[\frac{B_{3P}}{B_{el}}\phi_P(x_P)F_{val}^P(\beta,Q^2)\right.$$

$$\left.+f_P(x_P)F_{sea}^P(\beta,Q^2)\right]$$
(23)

and is different[4,5] from the mass spectrum in the forward ($t=0$) dissociation for the appearance of the factor $B_{3P}/B_{el}\approx1/2$ in the first term in the right-hand side of (23).

## 5. DIFFRACTIVE CONTRIBUTION TO $F_2^D(x,Q^2)$

The total diffraction dissociation cross-section

$$\sigma_D=\int dt dM^2\frac{d\sigma_D}{dt dM^2}$$

defines the diffractive contribution

$$F_2^D(x,Q^2)=\frac{Q^2}{4\pi^2\alpha_{em}}\sigma_D$$

to the proton structure function $F_2^D(x,Q^2)$,

$$F_2^D(x,Q^2)=\frac{\sigma_{tot}(pp)}{16\pi B_{3P}}\int_x^{x_P^c}\frac{dx_P}{x_P}\left[\frac{B_{3P}}{B_{el}}\phi_P(x_P)F_{val}^P\right.$$

$$\left.\times\left(\frac{x}{x_P},Q^2\right)+f_P(x_P)F_{sea}^P\left(\frac{x}{x_P},Q^2\right)\right],$$
(24)

where the numerical factor is $\sigma_{tot}(pp)/16\pi B_{3P}\approx0.3$ to an uncertainty $\lesssim25\%$ coming from the uncertainty in $B_{3P}$, which can eventually be reduced with the advent of the HERA measurements of $B_{3P}$. Here $x_P^c$ is subject to the experimental (pseudo)rapidity gap cutoff used to define the diffractive DIS, $\Delta\eta\gtrsim\Delta\eta_c\approx\log(1/x_P^c)$. In hadronic interactions with the recoil-proton tagging of diffraction dissociation, the pomeron exchange mechanism was shown to dominate for $x_P\lesssim x_P^c=0.05-0.1$. [17,28] The preliminary data from HERA correspond to a rather conservative cutoff $x_P^c\lesssim0.01$. [29,30]

In Fig. 5 we present our predictions for the diffraction structure function $F_2^D(x,Q^2)$. The strikingly weak $Q^2$-dependence of $F_2^D(x,Q^2)$ has its origin [4,14,31] in the fact that $F_{val}^P(\beta,Q^2)$ and $F_{sea}^P(\beta,Q^2)$ enter the integrand of (24) at large values of $\beta=x/x_P$ such that the predicted scaling violations, shown in Fig. 3, are still weak. Furthermore, the fluxes $\phi_P(x_P)$ and $f_P(x_P)$ rise towards small $x_P$, enhancing the contribution from large $\beta$ and further reducing the $Q^2$ dependence of $F_2^D(x,Q^2)$. We predict a steep rise of the diffractive structure function at large $1/x$, which comes predominantly from the rapid rise of the flux function $f_P(x_P)$. Figure 5 also shows the sensitivity of the predicted $F_2^D(x,Q^2)$ to the value of $x_P^c$ (the minimum rapidity gap $\Delta\eta_c$). We find a good agreement with the H1 estimate[30] for $F_2^D(x,Q^2)$. Notice that our calculation does not include the
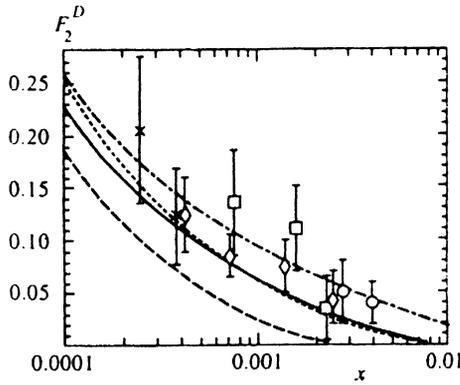
FIG. 5. Predictions from the dipole BFKL pomeron for the diffractive contribution $F_2^D(x,Q^2)$ to the proton structure function. The solid and dotted curves are for $x_P^c = 0.01$ and $Q^2 = 10$ and $Q^2 = 100$ GeV$^2$, respectively. The dashed and dash-and-dot curves are for $Q^2 = 10$ GeV$^2$ and rapidity-gap cuts $x_P^c = 0.003$ and $x_P^c = 0.03$, respectively. The data points are from the H1 experiment[30] for $Q^2 = 8.5$ (×), 15 (◊), 30 (□), 65 (○) GeV$^2$.

ing with the microscopic dipole BFKL pomeron. We demonstrated how the diffractive DIS cross-section can be factored into the flux of pomerons in the proton and the structure function of the pomeron. The Born approximation diffractive processes define the valence $q\bar{q}$ and valence gluon distributions, which serve as a nonperturbative input for a two-component structure function of the pomeron. These two components of the pomeron structure function enter the description of diffractive DIS with different fluxes of pomerons in the proton. The predicted breaking of the conventional parton-model factorization is strong and can be tested with higher precision data from HERA. Using the dipole BFKL cross-section which was earlier used for description of other several diffractive processes, we have presented parameter-free predictions for the pomeron structure function and for diffractive contribution to the proton structure function, which agree with the first experimental data from HERA.

It is worthwhile to notice that the two-component structure function of the pomeron is itself an approximation. For instance, the $x_P$- and $r$-dependence of the dipole cross-section $\sigma(x_P,r)$ do not factor,[2-5,11,15] and the dipole size $r \sim R_{val}(x_P)$, $R_{sea}(x_P)$, which makes the dominant contribution in (3) and (13) changes with $x_P$. Consequently, the span of the QCD evolution which is given[11,21] by $\log[Q^2 R_{val}^2(x_P)]$, $\log[Q^2 R_{sea}^2(x_P)]$, changes with $x_P$, breaking the factorization (7), (19) slightly. Numerically, in the region of $(x_P, Q^2)$ of interest at HERA, the variations of $R_{val}(x_P)$ and $R_{sea}(x_P)$ are still much smaller than the large difference between $R_{val}$ and $R_{sea}$ which is the origin of the two-component description. Because of the small $R_{sea}$, for $Q^2 \lesssim Q_P^2 = 10$ GeV$^2$, the $Q^2$-evolution of $F_{sea}^P(\beta,Q^2)$ can depart significantly from the GLDAP evolution.

A detailed description of transition from the photoproduction $Q^2 = 0$ to DIS will be presented elsewhere.

Further changes in this picture are possible beyond the subasymptotic region considered. At asymptotically large $1/\beta$, far beyond the reach of the HERA experiments, the
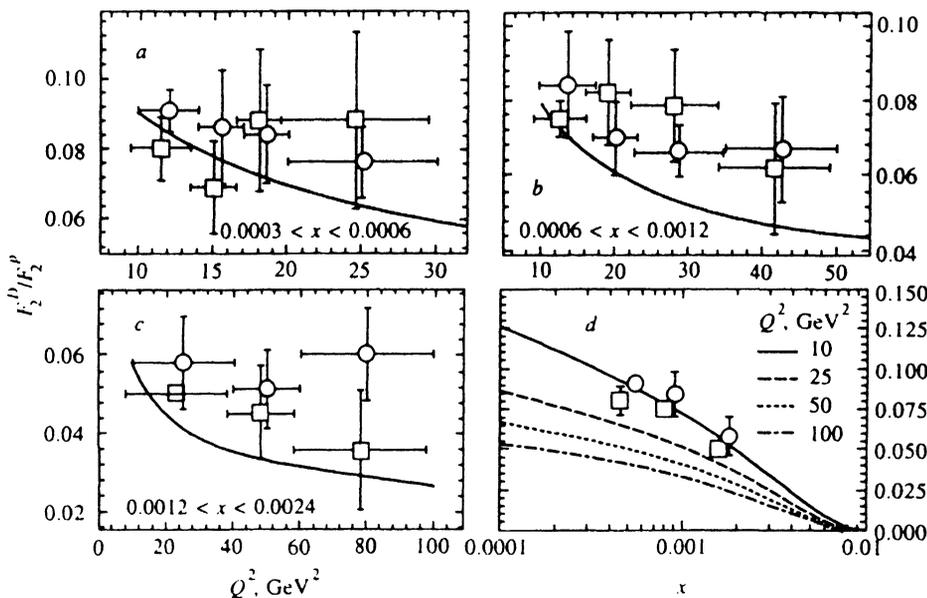
possible enhancement of the H1 and ZEUS values of $F_2^D(x,Q^2)$ for the unrejected diffraction excitation of protons into proton resonances and/or multiparticle states which escaped into the beam pipe. From the hadronic interaction data,[17] we can conclude that possible overestimation of $F_2^D(x,Q^2)$ by the H1 and ZEUS can not exceed 30% and presumably is smaller. Our results for the ratio $r_D(x,Q^2) = F_2^D(x,Q^2)/F_2^p(x,Q^2)$ are shown in Fig. 6. The steady decrease of $r_D(x,Q^2)$ with $Q^2$ was predicted in Refs. 4, 14 and comes mainly from the scaling violations in the proton structure function. The overall agreement with the H1[30] and ZEUS[32] results is good.

## 6. CONCLUSIONS AND DISCUSSION OF RESULTS

The purpose of this study has been to calculate the parton distributions in the pomeron at moderately small $\beta$, start-



FIG. 6. Predictions for the (a)-(c) $Q^2$-dependence and (d) $x$-dependence of the fraction $r_D(x,Q^2) = F_2^D(x,Q^2)/F_2^p(x,Q^2)$ of DIS on protons which goes via diffraction dissociation of photons for the rapidity-gap cut $x_P^c = 0.01$. The data points shown by squares and circles are from the H1[30] and ZEUS[32] experiments, respectively. The data points shown in the box (d) are for the lowest $Q^2$ bins in boxes (a)-(c).

LLQA ordering of sizes in higher order Fock states of the photon no longer dominates, and gluons of the exchanged pomerons will couple equally strongly to both soft and hard partons of the multiparton Fock state,[5] which may change the partonic structure of the cut pomeron.[11] Potentially, at least in the approximation $\alpha_S$=const sacrificing the asymptotic freedom of QCD, this region can be addressed in the formalism being developed in Ref 11; the numerical analysis and phenomenological implications of this formalism are as yet lacking.

Note added in press (20 July 1995):

After this paper was submitted for publication, the first measurements of the pomeron structure function and the flux of pomerons become available [H1 Collaboration: T. Ahmed, V. Andreev, B. Abrieu, et al., Phys. Lett. B **348**, 681 (1995); ZEUS Collaboration: M. Derrick, D. Kraukauer, S. Magill, et al., DESY-95-115 (June 1995)]. Good agreement with our predictions was found.

---

[1)]In Ref. 4, the factor $M^2$ was used instead of $M^2 + Q^2$ in the left-hand side of Eq. (1). Other conventions are possible,[2,3] but the observable cross-sections do not depend on how one factors them into the flux and structure function of the pomerons; we stick to the traditional Regge theory conventin.

[2)]Because of a different convention (see footnote 1), the structure function $F_{val}^P(\beta) = 0.25\beta(1 - \beta)^2$ of Eq. (50) in Ref. 4 contains the extra factor $1-\beta$, otherwise $F_{val}^P(\beta)$ of Ref. 4 is identical to $F_{val}^P(\beta)$ of the present paper.

---

[1]K. A. Ter-Martirosyan, Phys. Lett. B **44**, 179 (1973); A. B. Kaidalov and K. A. Ter-Martirosyan, Nucl. Phys. B **75**, 471 (1974).

[2]G. Ingelman and P. Schlein, Phys. Lett. B **152**, 256 (1985); H. Fritzsch and K. H. Streng, Phys. Lett. B **164**, 391 (1985); E. L. Berger, J. C. Collins, D. E. Soper, and G. Sterman, Nucl. Phys. B **286**, 704 (1987).

[3]A. Donnachie and P. V. Landshoff, Phys. Lett. B **191**, 309 (1987); Nucl. Phys. B **303**, 634 (1988).

[4]N. N. Nikolaev and B. G. Zakharov, Z. Phys. C **53**, 331 (1992).

[5]N. N. Nikolaev and B. G. Zakharov, Zh. Éksp. Teor. Fiz. **105**, 1117 (1994) [JETP **78**, 598 (1994)]; Z. Phys. C **64**, 631 (1994).

[6]N. N. Nikolaev, B. G. Zakharov, and V. R. Zoller, Pis'ma Zh. Éksp. Teor. Fiz. **59**, 8 (1994); N. N. Nikolaev, B. G. Zakharov, and V. R. Zoller, Phys. Lett. B **328**, 486 (1994); Zh. Éksp. Teor. Fiz. **105**, 1498 (1994) [JETP **78**, 806 (1994)].

[7]E. A. Kuraev, L. N. Lipatov, and V. S. Fadin. Zh. Éksp. Teor. Fiz. **71**, 840 (1976); **72**, 377 (1977) [Sov. Phys. JETP **44**, 443 (1976); **45**, 199 (1977)]; Ya. Ya. Balitsky and L. N. Lipatov Yad. Fiz. **28**, 1597 (1978) [Sov. J. Nucl.

Phys. **28**, 822 (1978)]; L. N. Lipatov, Zh. Éksp. Teor. Fiz. **90**, 1536 (1986) [Sov. Phys. JETP **63**, 904 (1986)]; L. N. Lipatov, [JETP Lett. **59**, 6 (1994)]; in *Perturbative Quantum Chromodynamics*, ed. by A. H. Mueller, World Science, Singapore (1989).

[8]A. Mueller and B. Patel, Nucl. Phys. B **425**, 471 (1994).

[9]N. N. Nikolaev and B. G. Zakharov, Phy. Lett. B **327**, 149, 157 (1994).

[10]N. N. Nikolaev and B. G. Zakharov, Phy. Lett. B **332**, 177 (1994).

[11]J. Bartels and M. Wüsthoff, DESY 94-016.

[12]J. Nemchik, N. N. Nikolaev, and B. G. Zakharov, Phys. Lett. B **341**, 228 (1994).

[13]V. N. Gribov and L. N. Lipatov, Sov. J. Nucl. Phys. **15**, 438 (1972); L. N. Lipatov, Yad. Fiz. **20**, 340 (1974) [Sov. J. Nucl. Phys. **20**, 181 (1974)]; Yu. L. Dokshitser, Zh. Éksp. Teor. Fiz. **73**, 1216 (1977) [Sov. Phys. JETP **46**, 641 (1977);]; G. Altarelli and G. Parisi, Nucl. Phys. B **126**, 298 (1977).

[14]N. N. Nikolaev and B. G. Zakharov, Z. Phys. C **49**, 607 (1991).

[15]ZEUS Collaboration: M. Derrick, D. Kraukaner, S. Magill et al., Phys. Lett. B **316**, 412 (1993); H1 Collaboration: I. Abt, T. Ahmed, V. Andreev et al., Nucl. Phys. B **407**, 515 (1993).

[16]V. Barone, M. Genovese, N. N. Nikolaev et al., Z. Phys. C **58**, 541 (1993).

[17]For reviews see e.g.: A. B. Kaidalov, Phys. Rep. **50**, 157 (1979); G. Alberi and G. Goggi, Phys. Rep. **74**, 1 (1981); K. Goulianos, Phys. Rep. **101**, 169 (1983).

[18]E. V. Shuryak, Rev. Mod. Phys. **65**, 1 (1993) (and references therein).

[19]M. Genovese, N. N. Nikolaev, and B. G. Zakharov, Zh. Éskp. Teor. Fiz., **108**, 1155 (1995) [JETP **81**, 633 (1995)]

[20]N. N. Nikolaev and B. G. Zakharov, Phys. Lett. B **332**, 184 (1994).

[21]B. Z. Kopeliovich and B. G. Zakharov, Phys. Rev. D **44**, 3466 (1991); O. Benhar, B. Z. Kopeliovich, Ch. Mariotti, N. N. Nikolaev, and B. G. Zakharov, Phys. Rev. Lett. **69**, 1156 (1992).

[22]B. Z. Kopeliovich, J. Nemchik, N. N. Nikolaev, and B. G. Zakharov, Phys. Lett. B **324**, 469 (1994).

[23]J. Nemchik, N. N. Nikolaev, and B. G. Zakharov, in *Proceedings of the Workshop on CEBAF at Higher Energies*, 14–16 March 1994, CEBAF, ed. by N. Isgur and P. Stoler, pp. 415–464.

[24]P. L. Frabetti, V. S. Paolone, P. M. Yaeger et al., Phys. Lett. B **316**, 197 (1993).

[25]NMC Collaboration: M. Arneodo, A. Arvidson, B. Badelek et al., Nucl. Phys. B **429**, 503 (1994).

[26]NMC Collaoration: M. Arneodo, A. Arvidson, B. Badelek et al., Phys. Lett. B **332**, 195 (1994).

[27]E665 Collaboration: M. R. Adams, S. Aid, P. L. Anthony et al., Phys. Rev. Lett. **74**, 1525 (1995).

[28]T. J. Chapin, R. L. Cool. K. Goulianos et al., Phy. Rev. D **31**, 17 (1985).

[29]ZEUS Collaboration: M. Derrick, D. Kraukauer, S. Magill et al., Phys. Lett. B **315**, 481 (1993).

[30]H1 Collaboration: T. Ahmed, V. Andreev, B. Andrieu et al., Nucl. Phys. B **429**, 477 (1994).

[31]N. N. Nikolaev, Oxford Univ. Preprint OU-TP **58/84** (1984); also in: Proc. VII Intern. Seminar on Problems of High Energy Physics, 19–26 June 1984; Dubna, USSR, pp. 174–182.

[32]ZEUS Collaboration: R. Devenish, Mini-School on Diffraction at HERA, DESY, May 4–7, 1994.